Characterization of Vif domains that mediate Feline Immunodeficiency Virus antagonism of APOBEC3-H and APOBEC3-CH restriction.

Olivia L. Sims[1, 2, 3-4#a], Ernest L. Maynard[5#b], and Eric M. Poeschla[1,2,6#c*]

[1]Department of Immunology, Mayo Graduate School, Mayo Clinic, Rochester, MN, United States of America

[2]Department of Molecular Medicine, Mayo Clinic College of Medicine, Mayo Clinic, Rochester, MN, United States of America

[3]Department of Virology and Immunology, Gladstone Institutes, San Francisco, CA, United States of America

[4]Department of Medicine, San Francisco General Hospital, University of California San Francisco, San Francisco, CA, United States of America

[5]Department of Biochemistry and Molecular Biology, Uniformed Services University of the Health Sciences, Bethesda, MD, United States of America

[6]Department of Medicine (Division of Infectious Diseases), Mayo Clinic College of Medicine, Mayo Clinic, Rochester, MN, United States of America

[*]Corresponding author

olivia.sims@ucsf.edu

[#a]Olivia L. Sims: Gladstone Institute of Virology and Immunology, Gladstone Institutes, San Francisco, CA; Department of Medicine, San Francisco General Hospital, University of California, San Francisco, CA, E-mail: olivia.sims@ucsf.edu.

[#b]Ernest L. Maynard: Protein Characterization, Analytical Development, Novavax Inc. Gaithersburg, MD, E-mail: ernie.maynard@gmail.com.

[#c]Eric M. Poeschla: Division of Infectious Diseases, University of Colorado School of Medicine, Aurora CO, E-mail: eric.poeschla@ucdenver.edu.

Abstract

Feline immunodeficiency virus (FIV) Vif mediates degradation of two anti-lentiviral feline APOBEC3 (fA3) proteins, fA3Z3 and fA3Z2bZ3. HIV-1 Vif targets the restriction factor human APOBEC3G (A3G, hA3Z2g-Z1c) for proteasome degradation to mediate viral evasion. Despite this similarity, FIV and HIV-1 Vif share limited homology. Vif binds hA3Z2g-Z1c through its N-terminal region, while its C-terminal region binds to an E3-ligase complex containing Cullin5 and Elongin B/C. Further, HIV-1 Vif contains critical domains in its C-terminus, including an adjacent BC box, the only shared domain between FIV and HIV-1 Vif, and a non-classical zinc finger (HCCH) domain. Felid lentivirus Vif, however, contains a highly conserved KCCC motif. While both Vifs have evolved to counteract select A3 antiretroviral proteins, the FIV Vif domains necessary to target fA3s for degradation are incompletely understood. To identify these domains, we used the well-characterized HIV-1 Vif domains to show that distinct mutations within the BC box of FIV Vif prevent fA3Z3 and fA3Z2bZ3 degradation and reduce virion infectivity. We also found that mutating any single residue in the KCCC motif blocked fA3 targeting and impaired FIV infectivity and replication. These mutations also failed to disrupt the FIV Vif and Cullin5 interaction. Further, we showed that, in contrast to the HCCH domain in HIV-1 Vif, the KCCC domain of FIV Vif does not bind zinc. However, unlike HIV-1 Vif, FIV Vif (C36 isolate) reduces intracellular levels of co-expressed Cullin5 proteins, a novel finding. Our results reveal important C-terminal residues in FIV Vif and show that the BC box and KCCC regions are critical for fA3 degradation, infectivity, and spreading replication.

Introduction

Lentiviruses cause chronic degenerative diseases in primate, ungulate, and feline species. The current AIDS pandemics in *Homo sapiens* and *Felis catus* are caused by human immunodeficiency virus type-1 (HIV-1) and feline immunodeficiency virus (FIV), respectively. All primate and non-primate lentiviruses encode a Vif protein, except the equine virus (1), that is essential for viral replication. HIV-1 Vif counters the antiviral activity of human APOBEC3G (A3G, hA3Z2g-Z1c) (2-11). In the absence of Vif, hA3Z2g-Z1c incorporates into virion particles of the virus-producing cell, where it inhibits viral replication by cytidine deamination of the viral minus–strand cDNA. This mechanism produces a plus-strand G-to-A hypermutation and interference during reverse transcription (4, 12-15).

A3 proteins, such as hA3Z2g-Z1c, are targeted to the proteasome for degradation (2, 16-22) via a Vif-dependent mechanism. The N-terminus of HIV-1 Vif, the ^{14}DRMR^{17} and ^{40}YHHY^{44} motifs (23-26), mediates the interaction with hA3Z2g-Z1c. However, the C-terminal region of Vif coordinates recruitment of a cellular E3 ligase complex consisting of Cullin5 (Cul5), Elongin C, Elongin B, an E2 ligase, and a Ring box (Rbx) protein (2, 5, 6, 18, 27). Recruitment of the E3 ligase occurs via several evolutionarily conserved domains in Vif, including a non-classical zinc-finger domain that binds to Cul5, SOCS (suppressors-of-cytokine-signaling-like domain) box, BC box, that interacts with Elongin C (2, 5-9, 15, 28-30), and a PPLP domain that interacts with Elongin B (1, 6, 31). While there are seven different human Cullin proteins (32, 33), HIV-1 Vif selectively interacts with Cul5 to stabilize the E3 ligase complex (2).

The half-life of both HIV-1 and simian immunodeficiency virus (SIV) Vif is stabilized and extended by core-binding factor-β (CBF-β) (34), which promotes the interaction between HIV-1/SIV Vif and Cul5 needed to form the E3-ligase complex (27, 35-39). The interface that mediates CBF-β binding to and stabilization of Vif were solved using the Vif/CBF-β/Cul5/Rbx2/EloBC and, separately, the Vif/CBF-β/N-terminal hA3Z2g-Z1c/EloBC complexes with X-ray crystallography and NMR spectroscopy, respectively (37, 40). CBF-β forms multiple interactions with the HIV-1 Vif N- and C-terminus, particularly with the BC box and HCCH domains (40-42). Mutating HCCH residues prevents the HIV-1 Vif/CBF-β/hCul5 interaction and significantly suppresses hA3Z2g-Z1c antiviral activity (41).

Non-primate mammals also encode antiviral APOBEC3 proteins (11, 43-50). Two *Felis catus* A3 proteins, fA3Z3 (fA3H) and fA3Z2bZ3 (fA3CH), restrict Δvif FIV (11, 43-46), a FIV vif-deletion mutant. FIV Vif promotes HIV-1 replication by mediating degradation of fA3Z3 or fA3Z2bZ3 when expressed in *cis* (45, 46) or *trans* (45) in Crandall-Rees Feline Kidney (CrFK) cells. FIV Vif also recruits an E3-ligase complex containing Cul5, EloC, and EloB (51). Although FIV Vif lacks the HCCH motif, a region adjacent to the BC box contains a strongly conserved KCCC motif (Fig. 1A) (45) that (45, 51) may serve as an atypical putative zinc-binding domain. Other lentiviral proteins contain an atypical zinc finger, such as the HIV-1 nucleocapsid (NC), that is important for transferring DNA intermediate strands during reverse transcription (52-54). Additionally, FIV Vif interacts with human and feline Cul5 (fCul5) (51); however, the residues governing the interaction between Vif and Cul5 are different between HIV-1 and FIV Vif. Indeed, replacing the two most C-terminal cysteine residues in the KCCC

106 motif of FIV Vif with serine (KCSS) no longer rescues ΔVif HIV-1 infectivity in the
107 presence of fA3 proteins, despite maintaining the interaction between FIV Vif and Cul5
108 (51).

109 The zinc chelator PTEN (N, N, N', N'-tetrakis-(2-pyridylmethyl)-ethylenediamine)
110 further distinguishes FIV from HIV-1. PTEN disrupts the interaction between HIV-1 Vif
111 and hCul5, but not between FIV Vif and fCul5, suggesting that FIV Vif might not be a
112 bona fide zinc-binding protein (9, 29, 51). However, PTEN can chelate iron and copper
113 (albeit it has a greater affinity for copper) and alter their cellular levels (55-57). While
114 earlier data suggested that FIV Vif does not bind zinc, biochemical data using purified
115 proteins were needed to verify this notion. Because HIV-1 NC has a non-canonical zinc
116 motif, we posited that the KCCC domain in FIV Vif might be the major zinc-binding site
117 and may mediate a functionally important Vif-Cul5 interaction. To test this hypothesis,
118 we interrogated the biomolecular interactions between FIV Vif and Cul5 using
119 isothermal titration calorimetry with and without zinc. Our studies were designed to
120 decipher whether FIV Vif is a zinc-binding protein and whether additional determinants
121 in the BC box and KCCC domain are essential for this interaction.

122
123
124

Materials and Methods

Cells

293T and CrFK cells were obtained from the American Type Culture Collection (ATCC). Cells were cultured in high-glucose Dulbecco's Modified Eagle Medium (DMEM) with 10% fetal bovine serum, 1% penicillin/streptomycin, and L-glutamine.

Plasmids

The expression plasmid containing codon-optimized wild-type (WT) FIV Vif C36 tagged with a hemagglutinin (HA) epitope (FIV C36 Vif-HA) was generated as previously described (45). Primer pairs (Table 1) were used for site-directed mutagenesis within FIV C36 HA-tagged Vif using sense and antisense primers to generate the following FIV Vif mutants: TLQ/AAA, TLQ/TAQ, A205L, A205S, A205T, K157R, C161S, and C187S. To generate the FIV Vif KCCC/RSSS mutant, a multisite-directed mutagenesis kit (Invitrogen) was used with two sense primers outlined in the primer table. Overlap-extension PCR deleted the KCCC domain using FIV C36 Vif-HA as a template with the outer sense (OS) and inner antisense (IAS) primers to generate the first PCR product. The second PCR reaction used the inner sense (IS) and outer antisense (OAS) primers. Combined PCR products were amplified with OS and OAS primers to generate ΔKCCC FIV C36 Vif-HA. PCR products were ligated into p1012 using EcoRI and KpnI restriction sites. The expression plasmid containing VR1012 human Cul5 Myc was a generous gift from Dr. Xiao Fang Yu at John Hopkins University School of Public Health (2).

Construction of expression plasmids containing fA3Z3 and fA3Z2bZ3 FLAG was previously described (45). The VR1012 feline Cul5 Myc was a generous gift of Dr. Yu (51). All expression plasmids were verified by Sanger DNA sequencing.

Table 1. Primer Sequences to Generate FIV Vif Expression Plasmids.

Name	Primer Sequences for FIV Vif Mutants
TLQ/AAA	5' TCTCCACCCGGCGCCGCCGCCCGCCTGGCCATG
	3' CATGGCCAGGCGGGCGGCGGCGCCGGGTGGAGA
TLQ/TAQ	5' CCACCCGGCACTGCCCAACGCCTGGCCATGCTGGCCTGTGGCC
	3' GGCCACAGGCCAGCATGGCCAGGCGTTGGGCAGTGCCGGGTGG
A205L	5' CCACCCGGCACTCTGCAACGCCTGCTGATGCTGGCCTGTGGCCGC
	3' GCGGCCACAGGCCAGCATCAGCAGGCGTTGCAGAGTGCCGGGTGG
A205S	5' CCACCCGGCACTCTGCAACGCCTGTCCATGCTGGCCTGTGGCCGC
	3' GCGGCCACAGGCCAGCATGGACAGGCGTTGCAGAGTGCCGGGTGG
A205T	5' CCACCCGGCACTCTGCAACGCCTGACCATGCTGGCCTGTGGCCGC
	3' GCGGCCACAGGCCAGCATGGTCAGGCGTTGCAGAGTGCCGGGTGG
K157R	5' GGCATGGTTGGTATCGCAATCCGCGCCTTCTCCTGCGGGGAGCGC
	3' GCGCTCCCCGCAGGAGAAGGCGCGGATTGCGATACCAACCATGCC
C161S	5' ATCGCAATCAAAGCCTTCTCCTCCGGGGAGCGCAAAATTGAAGCA
	3' TGCTTCAATTTTGCGCTCCCCGGAGGAGAAGGCTTTGATTGCGAT
C184S	5' GAAATTGATCCGAAAAAATGGTCCGGCGACTGCTGGAACCTGATG
	3' CATCAGGTTCCAGCAGTCGCCGGACCATTTTTTCGGATCAAT TTC
C187S	5' CCGAAAAAATGGTGCGGCGACTCCTGGAACCTGATGTGCCTGCGC
	3' GCGCAGGCACATCAGGTTCCAGGAGTCGCCGCACCATTTTTTCGG
KCCC/RSSS	5' GGTTGGTATCGCAATCCGCGCCTTCTCCTCCGGGGAGCGCAAAATTG
	5' GATCCGAAAAAATGGTCCGGCGACTCCTGGAACCTGATGTGC
ΔKCCC	*Overlap Extension Primers to Generate FIV Vif ΔKCCC Mutant*
OS	5' ATATATGAATTCCACCACACTGGACTAGTGGATCCATGGG
IAS	3'GCAGGCACATCAGGTTCCAGATTGCGATACCAACCATGCCCGGCCCCC AG
IS	5' GCATGGTTGGTATCGCAATCTGGAACCTGATGTGCCTGCGCAATTCTCC
OAS	3' ATATATGGTACCCATAGAGCCCACCGCATCCCCAGCATGC

Construction of Vif-Mutant Infectious Molecular Clones

Generation of 34TF10 C184S_187S Vif. The human cytomegalovirus driven infectious molecular clone 34TF10 (CT5) (58) containing a functional Orf2 was subcloned into pcDNA3.1(-) using EcoRI and KpnI (pcDNA3.1-CT5). pcDNA3.1-CT5 has a partial

158 fragment of Gag and full length Pol, Vif, and Orf2 genes (hereafter referred to as
159 pcDNA3.1-CT5Vif) (58). To introduce the C184_187S mutation into pcDNA3.1(-)
160 CT5Vif, the OS and IAS primers were used to generate the first PCR amplicon. The
161 second PCR product was synthesized with OAS and IS primers. Combined PCR
162 products were amplified with the OS and OAS primers, and the overlap product was
163 inserted into pCT5 with AccIII and KpnI.
164
165 **Creation of KCCC/RSSS.** To construct KCCC/RSSS, the C184_187S amplicon
166 described above was ligated into pcDNA3.1(-) empty vector using EcoRI and KpnI. To
167 generate KCCC/RSSS Vif, the pcDNA3.1-C184S_187S Vif plasmid and OS and IAS
168 primers were used to amplify the first PCR product. The pcDNA3.1-C184_187S plasmid
169 and OAS primer and the IS primers generated the second PCR amplicon. Combined
170 PCR products were amplified using OS and OAS primers to generate the CT5 Vif
171 KCCC/RSSS. The KCCC/RSSS PCR product was ligated into CT5 with AccIII and KpnI.
172
173 **Creation of 34TF10 TLQ/AAA Vif.** To generate the TLQ/AAA Vif mutant, the pcDNA
174 3.1-CT5 Vif plasmid and the OS and IAS primers were used to amplify the first PCR
175 product. The pcDNA3.1-CT5 Vif template and OAS and IS primers were used to amplify
176 the second PCR product. Combined PCR products were amplified with OS and OAS
177 primers to generate the TLQ/AAA amplicon. The TLQ/AAA PCR product was ligated
178 into CT5 with AccIII and KpnI.
179 **Creation of 34TF10 ΔKCCC_TLQ/AAA Vif.** To generate the ΔKCCC_TLQ/AAA Vif
180 mutant, the CT5 TLQ/AAA amplicon was ligated into pcDNA3.1(-) using EcoRI and

KpnI. The CT5 TLQ/AAA CT5 Vif template and OS and IAS primers were used to amplify the first PCR product. The second PCR product was amplified using the CT5 TLQ/AAA CT5Vif template DNA with OAS and IS primers. Combined PCR products were amplified using OS and OAS primers to generate the full-length ΔKCCC_TLQ/AAA Vif amplicon. The primers used to generate mutants with overlap-extension PCR are listed in Table 2. All mutants were verified by Sanger DNA sequencing.

Table 2. Overlap-Extension Primers to Generate Molecular Clones of Vif Mutant CT5.

Name	Mutant CT5 Primers Sequences
C184/187S	
OS	ATAT TCCGGATGAAAGAGAAAAGTATAAAAAAGAC
IAS	ACACATTAAATTCCATGAATCTCCTGACCATTTTTTTGGATC
IS	GATCCAAAAAAATGG TCA GGAGAT TCA TGGAATTTAATGTGT
OAS	ATAT GGTACC CTAAATGGGTTTACTCCTGGATTTAG
KCCC/RSSS	
OS	ATAT TCCGGATGAAAGAGAAAAGTATAAAAAAGAC
IAS	CTTTCTTTCGCCTGAACTAAAAGCGCGTATTGCTATACC
IS	GGTATAGCAATA CGC GCTTTTAGT TCA GGCGAAAGAAAG
OAS	ATAT GGTACCCTAAATGGGTTTACTCCTGGATTTAG
TLQ/AAA	
OS	ATAT TCCGGATGAAAGAGAAAAGTATAAAAAAGAC
IAS	CATAGCGAGTCTAGCAGCAGCCTTTGGAGGTG
IS	CACCTCCAAAGGCTGCTGCT AGACTCGCTATG
OAS	ATAT GGTACCCTAAATGGGTTTACTCCTGGATTTAG
ΔKCCC_TLQ/AAA	
OS	ATAT TCCGGATGAAAGAGAAAAGTATAAAAAAGAC
IAS	GTTTCTAAGACACATTAAATTCCATATTGCTATACCTACCATCC CTGGTCCCCAT
IS	GGATGGTAGGTATAGCAATATGGAATTTAATGTGTCTTAGAAACTCACC TCCAAAG
OAS	ATATGGTACC CTAAATGGGTTTACTCCTGGATTTAG

193 **Cloning, Expression and Purification of Recombinant FIV C36 Vif**

194 Expression constructs containing FIV C36 Vif (residues 156–200 and 156–213) were
195 generated by insertion into the EcoRI-Sbf I site of pMal c-5X (NEB). The resulting
196 mannose-binding protein (MBP)-Vif fusion proteins were expressed and purified as
197 previously described (59). Purified fusion proteins were concentrated in 20 mM HEPES
198 pH 7.4, 150 mM NaCl, and 200 µM Tris (2-carboxyethyl) phosphine and used
199 immediately for zinc-binding studies.

200

201 ITC Analysis of Zinc Binding to Recombinant FIV C36 Vif

202 Isothermal titration calorimetry (ITC) experiments were performed at 25°C using a
203 MicroCal iTC200 microcalorimeter (GE Healthcare) with a stirring rate of 1000 rpm.
204 Complete details of the ITC assay have been described (59). Briefly, purified FIV Vif
205 proteins were loaded into the ITC cell. A standardized stock solution of $Zn(NO_3)_2$ was
206 loaded in the ITC syringe and injected step-wise into the cell. After the first injection of
207 0.4 µl $Zn(NO_3)_2$, 19 additional injections of 2 µL were made into the cell at 2 minute
208 intervals to allow the system to return to equilibrium. Data were analyzed using
209 MicroCal Origin software.

210

211 Western Blotting

212 Following washing and trypsinization, cells lysates were obtained by suspending cell
213 pellets in a volume of 10 µl per 100,000 cells with protease inhibitor (Complete-Mini,
214 Roche) and an equivalent volume of 6X Laemmli buffer per sample. Lysates were
215 boiled and clarified. Proteins were resolved on a sodium dodecyl sulfate–polyacrylamide

electrophoresis (SDS-PAGE) gel and transferred to a polyvinylidene fluoride (PVDF) membrane (Thermo Scientific). Membranes were blocked in 10% milk and probed with primary antibodies. Membranes were incubated with appropriate secondary HRP-conjugated antibodies (dilutions 1: 5000–1:10000). Chemiluminescent substrates were used for visualization (Thermo Scientific 34080 or 34095).

Western Antibodies

Rat anti-HA (Roche, high-affinity clone 3F10), rabbit anti-HA (Santa Cruz), mouse anti-HA (Sigma H3663), polyclonal rabbit anti-Myc (Santa Cruz), rabbit anti-tubulin (Santa Cruz Product 9104), and mouse anti-Flag (Sigma F3165) antibodies were used at a dilution between 1:500 and 1:1000.

Proteasome Inhibition

Plasmid DNAs were transfected into 293T cells using calcium phosphate co-precipitation and medium was changed 12–16 hours later. Cells were treated with dimethyl sulfoxide (DMSO) or 10 □M MG132 (Sigma) 48 hours post-transfection, and cell lysates were harvested 22–24 hours later. Proteins were separated via SDS-PAGE as previously described.

Co-Immunoprecipitation

Co-transfections of 293T cells were performed as above. Transfection media was replaced with DMEM 12–16 hours later. Then, 48–52 hours post-transfection, cells were

washed with ice-cold PBS and lysed with ice-cold lysis buffer [150 mM NaCl, 50 mM TRIS HCl (pH 7.5), 1% Triton X, complete mini–protease inhibitor (Roche, Germany), and 200 mM phosphatase inhibitor (Sigma: Sodium Pervanadate)]. Sheep anti-mouse Immunoglobulin (Ig) magnetic dynabeads (sheep anti-mouse IgG, Invitrogen cat no.110.31; Oslo, Norway) were blocked with 0.01% bovine serum albumin (BSA) and 2 mM EDTA. Cell lysates were stored at -20ºC. To eliminate non-specific binding, beads were incubated with cell lysates at 4ºC for 1 hour. Beads from previous adsorption were discarded, and lysate were incubated with 1.0 µg mouse anti-HA antibody (Sigma H3663) to immunoprecipitate HA-tagged proteins. Pre-cleared lysates were incubated with 30 µl of pre-blocked dynabeads for 1 hour. Beads were washed three times with ice-cold co-immunoprecipitation lysis buffer. Immune complexes were eluted from beads with 30 µl of 2X β-mercaptoethanol Laemmli sample buffer and boiled at 95°C for 9 minutes. Proteins were separated by SDS-PAGE. Immunoblots were probed with a polyclonal rabbit antibody directed against the Myc epitope to assess the interaction between feline Cul5 Myc and FIV Vif HA-tagged (WT or mutant) proteins.

Immunofluorescence

The 293T cells were seeded onto Nunc LabTEK II chamber slides (Thermofisher, Catalog Number 154461). Adhered 293T cells were transfected with Fugene (Roche). Then, 48 hours post-transfection, cells were fixed with 4% formaldehyde, washed with PBS, and perforated with ice-cold methanol. Cells were stained with primary antibodies against HA- (high-affinity rat anti-HA antibody; Roche) or Myc- (rabbit anti-Myc; Santa Cruz) tagged proteins and probed with secondary antibodies goat anti-rabbit Alexa

Flour (AF) 488 or goat anti-rat AF 594 (Invitrogen) to analyze cellular distribution of proteins. Cells were stained with prolonged gold DAPI (Invitrogen) and mounted with a glass coverslip. All images were taken with a 510 laser-scanning confocal microscope (LSM 510).

Single-Cycle FIV-Replication Assays

The 293T producer cells were co-transfected using the calcium phosphate method with the following plasmids: transfer (FIV human cytomegalovirus (CMV)–driven luciferase reporter) (60), vesicular stomatitis virus glycoprotein (VSV-G), FP93 packaging (express FIV: gag, pol, and rev, but lacks Vif and envelope proteins) (61), fA3s (either fA3Z3 or fA3Z2bZ3), and codon-optimized FIV C36 Vif-HA (WT or mutant; or empty vector parental control) plasmids. Then, 16–20 hours post-transfection, media was changed; supernatants were collected with a 0.45 μM filter 32 hours later. Freshly plated 293T cells were transduced with equal amounts of virus normalized to reverse transcriptase (RT). Media was changed 16–20 hours after infection. Seventy-two hours post-infection, supernatants were removed, cells were washed with PBS, and then lysed with 1% Tween. Quantification of luciferase activity was measured by the relative light units emitted from each sample. Error bars reflect standard deviation from the mean.

Spreading Replication

The 293T producer cells were transfected with infectious molecular clones of WT or mutant 34TF10 Orf2 (CT5) using polyethylenimine (PEI) transfection reagent (Salk

Institute). To boost first-round infectivity, vesicular stomatitis virus glycoprotein G (VSV-G) was co-expressed during production. Media was changed 6–8 hours later. Viruses were harvested, filtered (0.45 μM), and pelleted on a 20% sucrose cushion 48 hours post-transfection. Viral titers were determined using a focal infectivity assay (FIA). Freshly plated CrFk cells were infected, and 12–16 hours later, they were washed thoroughly to eliminate input virus. Every 72 hours, viral supernatant was harvested. Simultaneously, feline cells were divided, cultured, and passaged with fresh media. The RT activity of viral supernatants was determined as previously described (62).

FIV Focal Infectivity Assay

The focal infectivity assay (FIA) assay has been previously described (63). In brief, CrFK cells were serially infected in 24-well plates. Sixteen hours post-infection, media was changed, and 40–42 hours post-infection, cells were washed and fixed with methanol. Cells were washed with 1X TNE (15.8 g Tris-HCl, 87 g NaCl, 7.44 g EDTA, 700 ml H_2O pH to 7.5.), blocked (1X TNE, 10% FBS), and probed with PPR antisera (a generous gift from Peggy Barr) and goat anti-cat HRP secondary antibody (MP Biomedicals 55293). Cells were stained with aminoethyl carbazol (AEC Sigma A-6926) solution to visualize infected cells. Infected cells were counted with a hemocytometer to empirically determine the viral titer.

Results

Vif mutations affect fA3 protein degradation

Given that fA3Z2bZ3 is more active than fA3Z3 in preventing Vif FIV replication (44-46), we used fA3Z2bZ3 in the majority of our experiments. We initially tested fA3Z2bZ3 with FIV Vif C36 harboring mutations in the BC box (TLQ/AAA, TLQ/TAQ, A205L, A205S, and A205T) and KCCC motif (K162R, C166S, C189S, C192S, KCCC/RSSS, and ΔKCCC) (Fig 1*A* and 1*B*). Wild-type (WT) and mutant FIV Vif proteins had similar intracellular patterns (Fig 1*C*) and expression levels (Fig 1*D*). In contrast, BC-box mutants TLQ/AAA, TLQ/TAQ, and A205L lost A3-degradative function (Fig 2*A* and *B*), while A205S and A205T maintained their function. Moreover, all KCCC mutants failed to direct fA3 degradation (Fig 2*C* and 2*D*). Treatment with the proteasome inhibitor MG132 partially rescued degradation of FIV Vif–mediated fA3Z2bZ3 and HIV-1 Vif–mediated hA3Z2g-Z1c (Fig 2*E* and 2*F*). Notably, Vif was poorly expressed when co-transfected with fA3Z2bZ3 and hA3Z2g-Z1c in DMSO-treated cells (Fig 2*E*). These findings suggest that Vif might be degraded when complexed with A3 proteins, consistent with rapid turnover of Vif and concomitant degradation when associated with A3 proteins (51, 64).

Fig 1. Vif protein alignments, mutations, cellular locations and expression levels. *A*, Amino-acid alignment of the C-terminus of HIV, SIVagm, and FIV Vif. *B*, FIV Vif C36 mutants. *C*, 293T cells were transfected with HA-tagged wild-type (WT) or mutant Vif with or without FLAG-tagged fA3Z2bZ3. Cells were subjected to immunofluorescence with antibodies to the respective epitope tags to visualize the cellular distribution of FIV Vif or fA3Z2bZ3 proteins alone (top row, left column) or together. Cellular DNA was

stained with DAPI. *D*, Immunoblots demonstrating equivalent expression of HA-tagged FIV Vif mutants.

Vif mutations influence viral infectivity

To determine whether loss of fA3 degradation correlates with increased restriction, we produced a virus containing a Δ*vif* FIV reporter both with and without fA3Z2bZ3 and the various Vif proteins. Consistent with their ability to target fA3Z2bZ3 for degradation (Fig 2*A*), A205S and A205T rescued FIV infectivity by 50% in the presence of fA3Z2bZ3 (Fig 3*A*). In contrast, TLQ/AAA, TLQ/TAQ, and A205L reduced FIV infectivity by 80% in the presence of fA3Z2bZ3 (Fig 3*A*). None of the KCCC mutants counteracted fA3Z2bZ3's antiviral activity (Fig 3*B*). We confirmed the correlation between fA3 levels and infectivity with immunoblotting (Fig 3*A* and 3*B*). These data reveal novel residues within the BC box (TAQ, A205L, A205S, and A205T) and KCCC domain (K162R, C166S, C189S, C192S, KCCC/RSSS, and ΔKCCC) that are required for FIV Vif activity against fA3s and viral infectivity.

Fig 2. Effects of FIV Vif mutations on fA3 protein degradation. *A* and *B*, Specific FIV Vif BC-box mutants target fA3s for destruction. 293T cells were co-transfected with 0.5 μg untagged p1012, wild-type (WT) or mutant FIV Vif HA, and 1 μg of untagged pcDNA3.1(-) or FLAG-tagged fA3 (fA3Z3 or fA3Z2bZ3). Protein separation was analyzed by SDS-PAGE. Immunoblot membranes were probed with antibodies recognizing HA, FLAG, or tubulin proteins. *C* and *D*, FIV Vif with mutations in the BC box were unable to target fA3s for degradation. 293T cells were co-transfected with or

without fA3s or untagged parental empty vectors with similar ratios of plasmid DNA as detailed in Fig 2*A* and 2*B*. A separate set of experiments showed FIV Vif mediates fA3Z2bZ3 proteasomal degradation. *E* and *F*, 293T cells were co-transfected with 0.5 μg of p1012 and 1 μg fA3Z2bZ3 or pcDNA3.1 (-) hA3Z2g-Z1c expression plasmids with 0.5 μg of WT FIV Vif or HIV-1 Vif with DMSO or MG132.

Fig 3. Effects of FIV Vif mutants on fA3CH restriction. *A* and *B,* Reporter viruses containing FIV ΔVif were produced in 293T cells transfected with 0.4 μg transfer vector, 0.2 μg pFP93 (FIV Gag-Pol and Rev) packaging vector, 0.2 μg pMD.G (VSV-G), with or without 0.3 μg of fA3Z2bZ3-FLAG and/or 0.5 μg Vif-HA [wild-type (WT) or mutant] plasmids, or the empty p1012 parental plasmid. The reverse transcription (RT) activity of each viral supernatant was determined, and equivalent amounts of RT-normalized virus were used to infect freshly plated 293T cells. Seventy-two hours after infection, lysates were analyzed for luciferase activity in triplicate. Standard deviation between triplicate samples was determined. FIV alone was set as 100%.

Vif mutations alter spreading replication

We then introduced four Vif mutants (KCCC/RSSS, ΔKCCC+TLQ/AAA, TLQ/AAA, and C184+187S) into the full-length CT5 molecular clone to determine their effects on spreading viral replication. We chose these mutants because all of the KCCC mutants were defective for single-round infectivity. Stocks of mutant FIV virus were produced in 293T cells and tested in CrFk cells. All four mutants exhibited similar reverse transcriptase (RT) activities (Fig 4*A*), as 293T cells lack antiviral hA3 activity, and they

did not negatively impact the infectious titer of the viruses (Fig 4*B*). Next, we infected CrFK cells with WT or mutant viruses at MOIs of 0.01 and 0.1. None of the four mutant viruses could replicate, while the WT virus replicated at 0.01 MOI, with large amounts of RT activity at 0.1 MOI (Fig 4*C* and 4*D*).

Fig 4. Effects of FIV Vif mutants block spreading replication of FIV. 293T producer cells were transiently transfected with VSVG-pseudotyped wild-type (WT) FIV or FIV Vif–mutant molecular clones (pCT5-based). *A* and *B*, Reverse transcription (RT) activity of viral supernatants and titers. *C* and *D*, Spreading replication: 4.5 x 10^4 CrFK cells were infected at two different MOIs (0.01 and 0.1). Every 72 hours, viral supernatant was collected and stored at -80°C until RT activity was determined.

Mutant Vif proteins co-localize and interact with feline Cul5

To date, the intracellular distribution of feline Cul5 (fCul5) has not been well characterized. Using confocal microscopy, we found fCul5 predominately in the cytoplasm, similar to Vif (Fig 5*A*). The KCCC mutants also display a slight intra-nuclear presence, in agreement with HIV-1 Vif, which has been shown to have a minimal Vif nuclear localization (65, 66). Co-immunoprecipitation studies assessed which FIV Vif domains were responsible for the interaction with Cul5. While the KCCC mutants interacted with fCul5 (Fig 5*C*, lanes 6–7), the TLQ/AAA mutant interacted poorly with fCul5 (Fig 5*C*, lane 8), as previously reported (51). Notably, when WT or mutant FIV Vif was co-expressed with fCul5 or hCul5, Cul5 expression significantly decreased (Fig 5*B*, lanes 5–8). As a result, less FIV Vif proteins were immunoprecipitated (Fig 5*C*, lanes 5–

8), an effect not observed if hCul5 and HIV-1 Vif are co-expressed (Fig 5*B,* lane 4). Despite multiple attempts, we were unable to detect an interaction between feline Elongin B and C (fEloB and fEloC, respectively) in the presence of FIV Vif and fCul5. The latter may be due to reduced Cul5, which could have limited detection of the FIV Vif/E3 ligase constituents (e.g., fEloB and fEloC). Nonetheless, with these data, we verified the FIV Vif/fCul5 interaction reported by Wang and colleagues (51).

Fig 5. The FIV Vif KCCC domain does not mediate fCul5 interaction. *A*, 293T cells were co-transfected with 1 μg feline Cul5-Myc plasmid and 1 μg wild-type (WT) or mutant FIV Vif-HA plasmid using PEI. Then, 48 hours later, cells were immunolabeled and imaged using confocal microscopy. *B*, Cell lysates from 293T cells co-transfected with 3 μg of each expression plasmid were analyzed 48 hours post-transfection *C*, Protein-protein interactions. Lysates were immunoprecipitated with mouse anti-HA, and then incubated with sheep anti-mouse beads. Immune complexes were eluted and subjected to SDS-PAGE. Immunoblots were probed with a rabbit anti-Myc antibody to evaluate the interaction between fCul5-Myc and WT or mutant FIV Vif-HA proteins.

Analysis of zinc binding to FIV Vif

A HCCH C-terminal motif in primate Vif proteins binds zinc and is required for Cul5 recognition. Feline Vifs have a similarly positioned KCCC motif. With isothermal titration calorimetry (ITC), we evaluated whether the KCCC domain of FIV Vif also binds zinc (59). FIV Vif proteins (Fig 6A) were expressed (Fig 6*B*) from the pMal-c5X vector and purified. All mannose binding protein (MBP)-Vif constructs showed no evidence of

417 protein degradation (Fig 6*B*). Further, with size-exclusion chromatography, we
418 separated and determined the protein quality of the purified MBP-Vif mutants. Notably,
419 most of the N-terminal constructs did not bind to the amylose resin, suggesting that they
420 may have formed aggregates that were unable to bind to the matrix (Fig 6*C*). Only two
421 MBP-Vif mutants were monomeric (Fig 6*D* and 6*E*), as the rest formed aggregates (Fig
422 6*D*). Because protein aggregates can impair the biological function of a protein (67), the
423 monomeric peaks that contained the intact KCCC-domain and BC-box motifs (156–
424 213), as well as the domain that lacks the BC-box motif (156–200), were collected,
425 concentrated, and analyzed further by ITC.
426
427 **Fig 6. Expression, Purification, and Size Exclusion of FIV Vifs.** *A*, Schematic map
428 and numbering of purified and codon-optimized FIV_{C36} Vif. *B*, Expression of pre- and
429 post-induction samples analyzed by SDS-PAGE. *C*, Verification of size exclusion
430 chromatography SEC elutant and supernatant alongside pre- and post-induction
431 samples were analyzed by SDS-PAGE. For each construct, the first lane is the induced
432 (I) sample from Fig 6*B*, the second lane is the supernatant (S), the third lane is the
433 unbound (U) flow-thru from the amylose column, and the fourth lane is the protein that
434 bound (B) to and was eluted from the amylose column. *D*, Table of elution volumes and
435 folding status of purified Vif MBP proteins. *E*, Monomeric resolution of purified Vif
436 proteins (156–213 and 156–200) at 17 mL.
437
438 MBP-Vif proteins were concentrated in buffer containing excess reductant (tris-
439 carboxyethyl phosphine) to maintain Cys residues in the thiol state. These thermogram

data indicate that zinc failed to bind to either FIV Vif construct (Fig 7*A* and 7*B*), consistent with a recent study in which the zinc chelator PTEN failed to inhibit fA3 degradation by FIV Vif (51). These results suggest that FIV Vif must degrade fA3 proteins via a mechanism distinct from that of the zinc-binding primate Vif.

Fig 7. Isothermal titration calorimetry data for zinc titrations into FIV C36 Vif. *A* and *B,* Integrated heat data for MBP-Vifs (156–200 and 156–213, respectively).

Discussion

With our data, we revealed novel residues within the FIV Vif BC box and KCCC domain that are required for infectivity and fA3 degradation. We also verified that the KCCC domain does not mediate the interaction with Cul5. In addition, we showed that FIV Vif does not bind zinc, and we are the first to demonstrate that FIV Vif (C36) targets human or feline Cul5 for degradation by an unknown mechanism. Interestingly, this phenomenon does not occur with HIV-1 Vif. These results collectively highlight a complex interplay between antiviral fA3 proteins, FIV Vif, and Cul5 that impacts FIV infectivity and replication.

Cullin proteins have an elongated structure that supports their conformational flexibility and facilitates binding to a broad range of substrate adaptors, including Vif. Vif usurps the host's E3-ligase complex (which contains Cul5, Rbx, E2, Elongin B, and Elongin C) to steer A3 proteins to the proteasome. HIV-1 Vif contains a HCCH domain that coordinates zinc binding and mediates hCul5 binding (4, 8, 17, 19). However, the domain of FIV Vif that interacts with the fCul E3 ligase to target the two active anti-FIV fA3 proteins (fA3Z3 and fA3Z2bZ3) is not known (11). We hypothesized that residues in the KCCC motif, which has a similar location and composition as the HCCH motif in HIV-1 Vif, would bind to Cul5.

Prior to our studies, it was unknown whether introducing the BC box and KCCC mutants would disrupt the cytoplasmic distribution of Vif. Toward this end, we performed confocal microscopy, which showed that the KCCC and BC-box mutants were stably expressed (Fig 1*D*) and predominantly distributed in the cytoplasm (Fig 1*C*) with

fA3Z2bZ3 (Fig 1*C*). The mutants co-localized with fA3Z2bZ3 in the absence of a proteasome inhibitor (Fig 1*C*). We believe that these FIV Vif/fA3Z2bZ3 complexes represent non-degraded populations that are incompletely targeted by the proteasome (51). We also tested whether previously unreported residues within the FIV Vif BC box would function similarly to HIV-1 Vif. Our results showed that two FIV Vif BC residues, TLQ/TAQ and A205L, were unable to target fA3 proteins for degradation (Fig 2*A* and 2*B*) as well as the reported TLQ/AAA mutant (48, 51). Interestingly, the A205S mutant targeted fA3s and partially rescued infectivity (Fig 2*A*, 2*B* and 3*A*). These results are consistent with the analogous A149S in HIV-1 Vif, which supports HIV-1 infectivity and hA3Z2g-Z1c elimination (15). In contrast, A205T restored FIV infectivity (Fig 3*A*), unlike the analogous A149T mutation in HIV-1 Vif (15). KCCC-domain mutants did not rescue Δvif FIV infectivity in the presence of fA3Z2bZ3 (Fig 3*B*), which correlates with their inability to mediate fA3Z2bZ3 degradation in virus-producing cells (Fig 3*B*). Collectively, these data support that the cytoplasmic localization of Vif proteins was not perturbed by mutations in the BC box and KCCC domain. Further, we demonstrated that both domains are necessary for targeting fA3s for degradation and single-round infectivity. We also provide data that conserving the alanine at residue 205 significantly contributes to the ability of FIV Vif to target fA3s for degradation. This finding suggests that the contact interface between Vif and fA3 proteins may not exactly mimic those within HIV-1 Vif and should be further studied.

An earlier report by Wang and colleagues showed that a triple alanine mutation (TLQ/AAA) and a KCCC/KCSS mutation in FIV Vif were able to block Vif HIV-1 infectivity in human cells. Here, we aimed to determine the impact of FIV infectivity and

spreading replication in human and feline cells, respectively. When we expressed a single-cycle, vif reporter virus, FIV infectivity was incompletely restored, despite WT Vif being expressed in *trans*. Unfortunately, we found that studying FIV Vif complementation was technically challenging. In our hands, Δvif FIV infectivity in the presence of ectopically expressed Vif was only restored by 50–70%, despite multiple attempts to optimize the FIV packaging-VSVG-Vif-A3 plasmid ratios. Previous studies were able to complement Vif FIV infectivity with expression of WT Vif in *trans;* however, different FIV Vifs that were derived from distinct isolates and packaging vectors were used (44, 46). Further, Wang and colleagues restored Δvif HIV-1 infectivity with WT FIV Vif_{34TF10} expressed in *trans* (51), while we used FIV_{C36} Vif. These experimental differences may explain the variation in restoring FIV infectivity between studies. Moreover, our FIV Vif mutants abolished spreading replication in CrFK cells, with a significant delay in FIV replication kinetics compared to WT Vif. Our data support previous work showing that Δvif FIV mutants are unable to restore FIV infectivity relative to WT controls in studies of spreading replication (68, 69). Further, we observed similar delays in spreading replication in CrFKs compared to peripheral blood mononuclear cells (PBMCs) derived from domestic cats and co-cultured with CrFK cells infected with Δvif FIV (69). CrFK cells express all fA3 proteins; hence, the delay in spreading WT replication may have been due to the antiviral activity of fA3 proteins in the absence of Vif (70). In support of this, all Vif mutant viruses were replication-incompetent, and the block in replication was sustained over 18 and 40 days at two different MOI (Fig 4*C* and 4*D*). Based on these data, the KCCC domain and BC box residues contribute to the essential function of Vif activity to enable FIV replication. Although, we do not formally

show the mechanisms here, presumably our Vif mutants may be unable to overcome the restriction of fA3 proteins necessary to recruit an E3 ligase Cullin complex to steer these antiviral proteins to the proteasome.

Previously, localization of fCul5 was unknown. We found that fCul5 localizes to the cytoplasm, similar to hCul5 (Fig 5*A*), and that WT and mutant Vif proteins co-localize with Cul5 (Fig 5*A*). We determined that the BC-box mutant TLQ/AAA has a reduced interaction with fCul5 and examined whether the KCCC domain served as a binding motif for fCul5. By co-immunoprecipitation, we found that the KCCC mutants retained their ability to interact with fCul5 (Fig 5*C*), demonstrating that the KCCC motif is not required for the Vif-Cul5 interaction. While we cannot exclude that deleting the KCCC domain alters proper folding of FIV Vif, the KCCC/RSSS mutant produced similar results in that the KCCC/RSSS mutant retained its interaction with Cul5.

We verified that FIV Vif and fCul5 interact (Fig 5*B*, lane 5). Interestingly, we observed reduced fCul5 and hCul5 expression in the presence of WT and FIV Vif mutants, but not in the presence of HIV-1 Vif (Fig 5*B*, lanes 4–9). We consistently observed robust co-immunoprecipitation between HIV-1 Vif and hCul5 (Fig 5*C*). We suspect that an unidentified factor that is not expressed in fibroblasts may influence the stability of the FIV Vif/fCul5 complex.

Curiously, fCul5 and hCul5 are 99% homologous (51). However, Wang and colleagues did not observe reduced fCul5 expression in the presence of codon-optimized FIV_{34TF10} Vif in their interaction studies (51), as we showed with codon-optimized FIV_{C36} Vif in our co-immunoprecipitation studies (Fig 5*A*). Because the affinities of these protein-protein interactions are largely unknown, we question whether

these two Vif variants differ in their ability to interact with fCul5. hA3s and HIV-1 Vif require different binding motifs to interact with fA3s and FIV Vif (71). Further, Troy and colleagues showed that the pathogenicity of FIV depends on the Vif isolate (70), which might correlate with the interaction, or lack thereof, between FIV_{C36} Vif and fCul5. Thus, our results demonstrate that a single residue within the BC box, TLQ/TAQ or A205L, of FIV Vif can induce fA3Z3 and fA3Z2bZ3 degradation, and that the KCCC motif does not mediate the interaction between fCul5 and FIV Vif.

Lastly, our biochemical ITC data showed that the KCCC domain of FIV Vif does not bind zinc (Fig 7*B*). We were unable to express a purified form of the full-length FIV Vif protein (Fig 6*D*), because purifying Vif is technically challenging (37, 72, 73). Nonetheless, our finding that FIV Vif does not bind to zinc agrees with studies of the PTEN zinc chelator carried out by Wang and colleagues (51). However, this result contrasts with the zinc binding we observed for HIV-1 Vif using ITC (59). Zinc binding to HIV-1 Vif changes the protein conformation and promotes interaction with Cul5. In the case of FIV Vif, such a conformational change is either not required or driven by other processes. Curiously, non-primate lentiviral BIV Vif requires zinc and has a novel zinc-binding domain, C-x1-C-x1-H-x19-C. Visna Vif, however, does not use zinc for its activity, but rather relies on a novel protein-protein interaction (74, 75).

While we were preparing this manuscript, Kane and colleagues showed that FIV_{34TF10} Vif interacts with both hCul2 and hCul5, albeit its binding to hCul2 requires the Vif N-terminal tag (75). Recruitment of Cul5 is mediated by the N-terminus of HIV-1 Vif (76), and stabilization between primate Vifs and Cul5 requires CBF-β, which targets hA3Z2g-Z1c for proteasomal degradation (27, 39, 72). Interestingly, FIV Vif does not

require CBF-β to stabilize Vif, form the fE3-ligase complex, or mediate fA3-mediated degradation (39, 75), despite the identical homology between feline and human CBF-β (75). A non-primate Visna Vif has evolved to use a novel cellular co-factor, Cylophilin A, to promote the Visna Vif/Cul2 E3-ligase complex needed to degrade ovine A3 proteins, whereas BIV Vif does not require a co-factor to eliminate bovine A3 via the proteasome (75).

These studies illustrate the complex selection criteria that lentiviruses have undergone to allow species-specific Vif to adapt to host A3 proteins (71, 75, 77, 78). We hypothesize that the domestic cat may have flexible fCul2/fCul5 usage, unlike HIV-1 Vif, which predominantly interacts with hCul5. The reported study by Kane and colleagues focused on the FIV Vif–host interactome in human 293T cells (75). However, further studies in feline cells should determine whether Vif preferentially binds fCul2 or fCul5, examine if other feline Cullins interact with FIV Vif, and identify the elusive cellular co-factor that stabilizes FIV Vif. Based on our results, we believe that the lentiviral/host interactome hijacks novel cellular co-factors needed to eliminate the antiviral properties of A3 proteins, as is the case with FIV Vif, despite 100% homology between human and feline CBF-β (75). Data from these studies may serve as a platform for future experiments to provide mechanistic insight important for the development of novel antiviral HIV-1 therapies.

Acknowledgments. We thank Dyana Saenz, and Mary Peretz for technical assistance and advice; Anne Meehan, James Morrison, and Hind Fadel for advice; Xiao Fang Yu (Johns Hopkins) and Jiawen Wang (Jilin University) for expression plasmids; and P. Barr (Western University of Health Sciences) for antisera. Supported by NIH AI100797.

References

1. Oberste MS, Gonda MA. Conservation of amino-acid sequence motifs in lentivirus Vif proteins. Virus Genes. 1992;6(1):95-102.
2. Yu X, Yu Y, Liu B, Luo K, Kong W, Mao P, et al. Induction of APOBEC3G ubiquitination and degradation by an HIV-1 Vif-Cul5-SCF complex. Science. 2003;302(5647):1056-60.
3. Yu Q, Konig R, Pillai S, Chiles K, Kearney M, Palmer S, et al. Single-strand specificity of APOBEC3G accounts for minus-strand deamination of the HIV genome. Nat Struct Mol Biol. 2004;11(5):435-42.
4. Sheehy AM, Gaddis NC, Choi JD, Malim MH. Isolation of a human gene that inhibits HIV-1 infection and is suppressed by the viral Vif protein. Nature. 2002;418(6898):646-50.
5. Mehle A, Goncalves J, Santa-Marta M, McPike M, Gabuzda D. Phosphorylation of a novel SOCS-box regulates assembly of the HIV-1 Vif-Cul5 complex that promotes APOBEC3G degradation. Genes Dev. 2004;18(23):2861-6.
6. Luo K, Xiao Z, Ehrlich E, Yu Y, Liu B, Zheng S, et al. Primate lentiviral virion infectivity factors are substrate receptors that assemble with cullin 5-E3 ligase through a HCCH motif to suppress APOBEC3G. Proc Natl Acad Sci U S A. 2005;102(32):11444-9.
7. Xiao Z, Ehrlich E, Yu Y, Luo K, Wang T, Tian C, et al. Assembly of HIV-1 Vif-Cul5 E3 ubiquitin ligase through a novel zinc-binding domain-stabilized hydrophobic interface in Vif. Virology. 2006;349(2):290-9.
8. Mehle A, Thomas ER, Rajendran KS, Gabuzda D. A zinc-binding region in Vif binds Cul5 and determines cullin selection. J Biol Chem. 2006;281(25):17259-65.
9. Xiao Z, Ehrlich E, Luo K, Xiong Y, Yu XF. Zinc chelation inhibits HIV Vif activity and liberates antiviral function of the cytidine deaminase APOBEC3G. FASEB J. 2007;21(1):217-22.
10. Chiu YL, Greene WC. The APOBEC3 cytidine deaminases: an innate defensive network opposing exogenous retroviruses and endogenous retroelements. Annu Rev Immunol. 2008;26:317-53.
11. LaRue RS, Andresdottir V, Blanchard Y, Conticello SG, Derse D, Emerman M, et al. Guidelines for naming nonprimate APOBEC3 genes and proteins. J Virol. 2009;83(2):494-7.
12. Mangeat B, Turelli P, Caron G, Friedli M, Perrin L, Trono D. Broad antiretroviral defence by human APOBEC3G through lethal editing of nascent reverse transcripts. Nature. 2003;424(6944):99-103.
13. Mariani R, Chen D, Schrofelbauer B, Navarro F, Konig R, Bollman B, et al. Species-specific exclusion of APOBEC3G from HIV-1 virions by Vif. Cell. 2003;114(1):21-31.
14. Zhang H, Yang B, Pomerantz RJ, Zhang C, Arunachalam SC, Gao L. The cytidine deaminase CEM15 induces hypermutation in newly synthesized HIV-1 DNA. Nature. 2003;424(6944):94-8.

15. Yu Y, Xiao Z, Ehrlich ES, Yu X, Yu XF. Selective assembly of HIV-1 Vif-Cul5-ElonginB-ElonginC E3 ubiquitin ligase complex through a novel SOCS box and upstream cysteines. Genes Dev. 2004;18(23):2867-72.
16. Conticello SG, Harris RS, Neuberger MS. The Vif protein of HIV triggers degradation of the human antiretroviral DNA deaminase APOBEC3G. Curr Biol. 2003;13(22):2009-13.
17. Marin M, Rose KM, Kozak SL, Kabat D. HIV-1 Vif protein binds the editing enzyme APOBEC3G and induces its degradation. Nat Med. 2003;9(11):1398-403.
18. Sheehy AM, Gaddis NC, Malim MH. The antiretroviral enzyme APOBEC3G is degraded by the proteasome in response to HIV-1 Vif. Nat Med. 2003;9(11):1404-7.
19. Stopak K, de Noronha C, Yonemoto W, Greene WC. HIV-1 Vif blocks the antiviral activity of APOBEC3G by impairing both its translation and intracellular stability. Mol Cell. 2003;12(3):591-601.
20. Mehle A, Strack B, Ancuta P, Zhang C, McPike M, Gabuzda D. Vif overcomes the innate antiviral activity of APOBEC3G by promoting its degradation in the ubiquitin-proteasome pathway. J Biol Chem. 2004;279(9):7792-8.
21. Kobayashi M, Takaori-Kondo A, Miyauchi Y, Iwai K, Uchiyama T. Ubiquitination of APOBEC3G by an HIV-1 Vif-Cullin5-Elongin B-Elongin C complex is essential for Vif function. J Biol Chem. 2005;280(19):18573-8.
22. Mercenne G, Bernacchi S, Richer D, Bec G, Henriet S, Paillart JC, et al. HIV-1 Vif binds to APOBEC3G mRNA and inhibits its translation. Nucleic Acids Res. 2010;38(2):633-46.
23. Simon V, Zennou V, Murray D, Huang Y, Ho DD, Bieniasz PD. Natural variation in Vif: differential impact on APOBEC3G/3F and a potential role in HIV-1 diversification. PLoS Pathog. 2005;1(1):e6.
24. Tian C, Yu X, Zhang W, Wang T, Xu R, Yu XF. Differential requirement for conserved tryptophans in human immunodeficiency virus type 1 Vif for the selective suppression of APOBEC3G and APOBEC3F. J Virol. 2006;80(6):3112-5.
25. Russell RA, Pathak VK. Identification of two distinct human immunodeficiency virus type 1 Vif determinants critical for interactions with human APOBEC3G and APOBEC3F. J Virol. 2007;81(15):8201-10.
26. Schrofelbauer B, Senger T, Manning G, Landau NR. Mutational alteration of human immunodeficiency virus type 1 Vif allows for functional interaction with nonhuman primate APOBEC3G. J Virol. 2006;80(12):5984-91.
27. Jager S, Kim DY, Hultquist JF, Shindo K, LaRue RS, Kwon E, et al. Vif hijacks CBF-beta to degrade APOBEC3G and promote HIV-1 infection. Nature. 2012;481(7381):371-5.
28. Giri K, Scott RA, Maynard EL. Molecular structure and biochemical properties of the HCCH-Zn2+ site in HIV-1 Vif. Biochemistry. 2009;48(33):7969-78.
29. Paul I, Cui J, Maynard EL. Zinc binding to the HCCH motif of HIV-1 virion infectivity factor induces a conformational change that mediates protein-protein interactions. Proc Natl Acad Sci U S A. 2006;103(49):18475-80.
30. Stanley BJ, Ehrlich ES, Short L, Yu Y, Xiao Z, Yu XF, et al. Structural insight into the human immunodeficiency virus Vif SOCS box and its role in human E3 ubiquitin ligase assembly. J Virol. 2008;82(17):8656-63.

676 31. Bergeron JR, Huthoff H, Veselkov DA, Beavil RL, Simpson PJ, Matthews SJ, et
677 al. The SOCS-box of HIV-1 Vif interacts with ElonginBC by induced-folding to recruit its
678 Cul5-containing ubiquitin ligase complex. PLoS Pathog. 2010;6(6):e1000925.
679 32. Petroski MD, Deshaies RJ. Function and regulation of cullin-RING ubiquitin
680 ligases. Nat Rev Mol Cell Biol. 2005;6(1):9-20.
681 33. Sarikas A, Hartmann T, Pan ZQ. The cullin protein family. Genome Biol.
682 2011;12(4):220.
683 34. Han X, Liang W, Hua D, Zhou X, Du J, Evans SL, et al. Evolutionarily conserved
684 requirement for core binding factor beta in the assembly of the human
685 immunodeficiency virus/simian immunodeficiency virus Vif-cullin 5-RING E3 ubiquitin
686 ligase. J Virol. 2014;88(6):3320-8.
687 35. Fribourgh JL, Nguyen HC, Wolfe LS, Dewitt DC, Zhang W, Yu XF, et al. Core
688 binding factor beta plays a critical role by facilitating the assembly of the Vif-cullin 5 E3
689 ubiquitin ligase. J Virol. 2014;88(6):3309-19.
690 36. Miyagi E, Kao S, Yedavalli V, Strebel K. CBFbeta enhances de novo protein
691 biosynthesis of its binding partners HIV-1 Vif and RUNX1 and potentiates the Vif-
692 induced degradation of APOBEC3G. J Virol. 2014;88(9):4839-52.
693 37. Guo Y, Dong L, Qiu X, Wang Y, Zhang B, Liu H, et al. Structural basis for
694 hijacking CBF-beta and CUL5 E3 ligase complex by HIV-1 Vif. Nature.
695 2014;505(7482):229-33.
696 38. Salter JD, Lippa GM, Belashov IA, Wedekind JE. Core-binding factor beta
697 increases the affinity between human Cullin 5 and HIV-1 Vif within an E3 ligase
698 complex. Biochemistry. 2012;51(44):8702-4.
699 39. Hultquist JF, Binka M, LaRue RS, Simon V, Harris RS. Vif proteins of human and
700 simian immunodeficiency viruses require cellular CBFbeta to degrade APOBEC3
701 restriction factors. J Virol. 2012;86(5):2874-7.
702 40. Kouno T, Luengas EM, Shigematsu M, Shandilya SM, Zhang J, Chen L, et al.
703 Structure of the Vif-binding domain of the antiviral enzyme APOBEC3G. Nat Struct Mol
704 Biol. 2015;22(6):485-91.
705 41. Wang H, Lv G, Zhou X, Li Z, Liu X, Yu XF, et al. Requirement of HIV-1 Vif C-
706 terminus for Vif-CBF-beta interaction and assembly of CUL5-containing E3 ligase. BMC
707 Microbiol. 2014;14:290.
708 42. Wang X, Wang X, Zhang H, Lv M, Zuo T, Wu H, et al. Interactions between HIV-
709 1 Vif and human ElonginB-ElonginC are important for CBF-beta binding to Vif.
710 Retrovirology. 2013;10:94.
711 43. Munk C, Zielonka J, Constabel H, Kloke BP, Rengstl B, Battenberg M, et al.
712 Multiple restrictions of human immunodeficiency virus type 1 in feline cells. J Virol.
713 2007;81(13):7048-60.
714 44. Munk C, Beck T, Zielonka J, Hotz-Wagenblatt A, Chareza S, Battenberg M, et al.
715 Functions, structure, and read-through alternative splicing of feline APOBEC3 genes.
716 Genome Biol. 2008;9(3):R48.
717 45. Stern MA, Hu C, Saenz DT, Fadel HJ, Sims O, Peretz M, et al. Productive
718 replication of Vif-chimeric HIV-1 in feline cells. J Virol. 2010;84(14):7378-95.
719 46. Zielonka J, Marino D, Hofmann H, Yuhki N, Lochelt M, Munk C. Vif of feline
720 immunodeficiency virus from domestic cats protects against APOBEC3 restriction
721 factors from many felids. J Virol. 2010;84(14):7312-24.

722 47. LaRue RS, Jonsson SR, Silverstein KA, Lajoie M, Bertrand D, El-Mabrouk N, et
723 al. The artiodactyl APOBEC3 innate immune repertoire shows evidence for a multi-
724 functional domain organization that existed in the ancestor of placental mammals. BMC
725 Mol Biol. 2008;9:104.
726 48. Larue RS, Lengyel J, Jonsson SR, Andresdottir V, Harris RS. Lentiviral Vif
727 degrades the APOBEC3Z3/APOBEC3H protein of its mammalian host and is capable of
728 cross-species activity. J Virol. 2010;84(16):8193-201.
729 49. Fadel HJ, Poeschla EM. Retroviral restriction and dependency factors in
730 primates and carnivores. Vet Immunol Immunopathol. 2011;143(3-4):179-89.
731 50. Fadel HJ, Saenz DT, Guevara R, von Messling V, Peretz M, Poeschla EM.
732 Productive replication and evolution of HIV-1 in ferret cells. J Virol. 2012;86(4):2312-22.
733 51. Wang J, Zhang W, Lv M, Zuo T, Kong W, Yu X. Identification of a Cullin5-
734 ElonginB-ElonginC E3 complex in degradation of feline immunodeficiency virus Vif-
735 mediated feline APOBEC3 proteins. J Virol. 2011;85(23):12482-91.
736 52. Guo J, Wu T, Anderson J, Kane BF, Johnson DG, Gorelick RJ, et al. Zinc finger
737 structures in the human immunodeficiency virus type 1 nucleocapsid protein facilitate
738 efficient minus- and plus-strand transfer. J Virol. 2000;74(19):8980-8.
739 53. Krishna SS, Majumdar I, Grishin NV. Structural classification of zinc fingers:
740 survey and summary. Nucleic Acids Res. 2003;31(2):532-50.
741 54. Laity JH, Lee BM, Wright PE. Zinc finger proteins: new insights into structural
742 and functional diversity. Curr Opin Struct Biol. 2001;11(1):39-46.
743 55. Haas KL, Franz KJ. Application of metal coordination chemistry to explore and
744 manipulate cell biology. Chem Rev. 2009;109(10):4921-60.
745 56. Hashemi M, Ghavami S, Eshraghi M, Booy EP, Los M. Cytotoxic effects of intra
746 and extracellular zinc chelation on human breast cancer cells. Eur J Pharmacol.
747 2007;557(1):9-19.
748 57. Sigdel TK, Easton JA, Crowder MW. Transcriptional response of Escherichia coli
749 to TPEN. J Bacteriol. 2006;188(18):6709-13.
750 58. Poeschla EM, Wong-Staal F, Looney DJ. Efficient transduction of nondividing
751 human cells by feline immunodeficiency virus lentiviral vectors. Nat Med. 1998;4(3):354-
752 7.
753 59. Ghimire-Rijal S, Maynard EL, Jr. Comparative thermodynamic analysis of zinc
754 binding to the His/Cys motif in virion infectivity factor. Inorg Chem. 2014;53(9):4295-
755 302.
756 60. Llano M, Saenz DT, Meehan A, Wongthida P, Peretz M, Walker WH, et al. An
757 essential role for LEDGF/p75 in HIV integration. Science. 2006;314(5798):461-4.
758 61. Loewen N, Barraza R, Whitwam T, Saenz DT, Kemler I, Poeschla EM. FIV
759 Vectors. Methods Mol Biol. 2003;229:251-71.
760 62. Saenz DT, Teo W, Olsen JC, Poeschla EM. Restriction of feline
761 immunodeficiency virus by Ref1, Lv1, and primate TRIM5alpha proteins. J Virol.
762 2005;79(24):15175-88.
763 63. de Parseval A, Chatterji U, Morris G, Sun P, Olson AJ, Elder JH. Structural
764 mapping of CD134 residues critical for interaction with feline immunodeficiency virus.
765 Nat Struct Mol Biol. 2005;12(1):60-6.
766 64. Baig TT, Feng Y, Chelico L. Determinants of efficient degradation of APOBEC3
767 restriction factors by HIV-1 Vif. J Virol. 2014;88(24):14380-95.

65. Chatterji U, Grant CK, Elder JH. Feline immunodeficiency virus Vif localizes to the nucleus. J Virol. 2000;74(6):2533-40.
66. Farrow MA, Somasundaran M, Zhang C, Gabuzda D, Sullivan JL, Greenough TC. Nuclear localization of HIV type 1 Vif isolated from a long-term asymptomatic individual and potential role in virus attenuation. AIDS Res Hum Retroviruses. 2005;21(6):565-74.
67. Tanaka M, Komi Y. Layers of structure and function in protein aggregation. Nat Chem Biol. 2015;11(6):373-7.
68. Shen X, Leutenegger CM, Stefano Cole K, Pedersen NC, Sparger EE. A feline immunodeficiency virus vif-deletion mutant remains attenuated upon infection of newborn kittens. J Gen Virol. 2007;88(Pt 10):2793-9.
69. Lockridge KM, Himathongkham S, Sawai ET, Chienand M, Sparger EE. The feline immunodeficiency virus vif gene is required for productive infection of feline peripheral blood mononuclear cells and monocyte-derived macrophages. Virology. 1999;261(1):25-30.
70. Troyer RM, Thompson J, Elder JH, VandeWoude S. Accessory genes confer a high replication rate to virulent feline immunodeficiency virus. J Virol. 2013;87(14):7940-51.
71. Zhang Z, Gu Q, Jaguva Vasudevan AA, Hain A, Kloke BP, Hasheminasab S, et al. Determinants of FIV and HIV Vif sensitivity of feline APOBEC3 restriction factors. Retrovirology. 2016;13(1):46.
72. Zhang W, Du J, Evans SL, Yu Y, Yu XF. T-cell differentiation factor CBF-beta regulates HIV-1 Vif-mediated evasion of host restriction. Nature. 2012;481(7381):376-9.
73. Reingewertz TH, Benyamini H, Lebendiker M, Shalev DE, Friedler A. The C-terminal domain of the HIV-1 Vif protein is natively unfolded in its unbound state. Protein Eng Des Sel. 2009;22(5):281-7.
74. Zhang J, Wu J, Wang W, Wu H, Yu B, Wang J, et al. Role of cullin-elonginB-elonginC E3 complex in bovine immunodeficiency virus and maedi-visna virus Vif-mediated degradation of host A3Z2-Z3 proteins. Retrovirology. 2014;11:77.
75. Kane JR, Stanley DJ, Hultquist JF, Johnson JR, Mietrach N, Binning JM, et al. Lineage-Specific Viral Hijacking of Non-canonical E3 Ubiquitin Ligase Cofactors in the Evolution of Vif Anti-APOBEC3 Activity. Cell Rep. 2015;11(8):1236-50.
76. Evans SL, Schon A, Gao Q, Han X, Zhou X, Freire E, et al. HIV-1 Vif N-terminal motif is required for recruitment of Cul5 to suppress APOBEC3. Retrovirology. 2014;11:4.
77. Ai Y, Zhu D, Wang C, Su C, Ma J, Ma J, et al. Core-binding factor subunit beta is not required for non-primate lentiviral Vif-mediated APOBEC3 degradation. J Virol. 2014;88(20):12112-22.
78. Yoshikawa R, Nakano Y, Yamada E, Izumi T, Misawa N, Koyanagi Y, et al. Species-specific differences in the ability of feline lentiviral Vif to degrade feline APOBEC3 proteins. Microbiol Immunol. 2016;60(4):272-9.

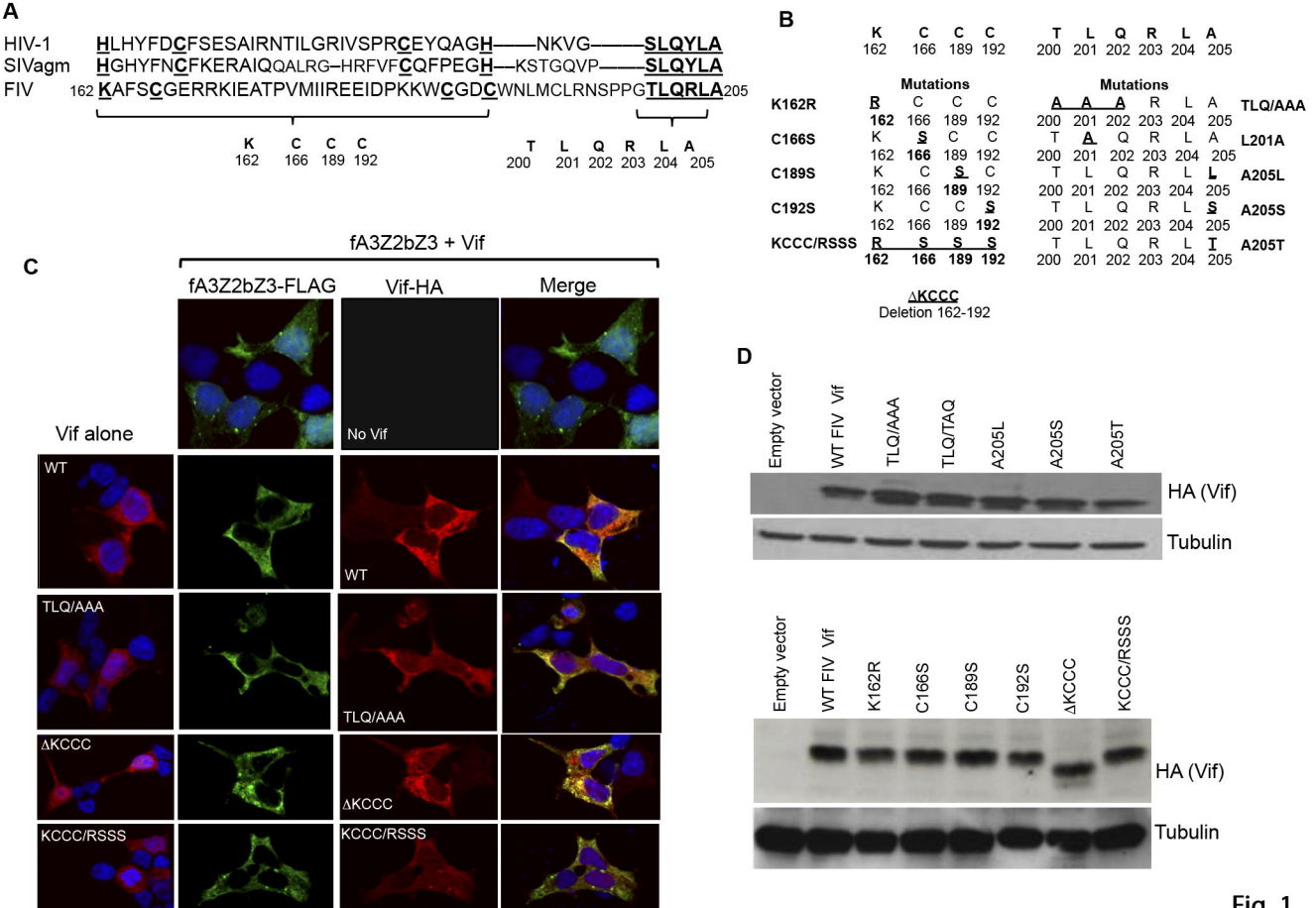
A
HIV-1 HLHYFDCFSESAIRNTILGRIVSPRCEYQAGH——NKVG——SLQYLA
SIVagm HGHYFNCFKERAIQQALRG–HRFVFCQFPEGH—KSTGQVP——SLQYLA
FIV 162 KAFSCGERRKIEATPVMIIREEIDPKKWCGDCWNLMCLRNSPPGTLQRLA205
K C C C T L Q R L A
162 166 189 192 200 201 202 203 204 205
B
K C C C T L Q R L A
162 166 189 192 200 201 202 203 204 205
Mutations
Mutations
K162R R C C C A A A R L A TLQ/AAA
162 166 189 192 200 201 202 203 204 205
C166S K S C C T A Q R L A L201A
162 166 189 192 200 201 202 203 204 205
C189S K C S C T L Q R L L A205L
162 166 189 192 200 201 202 203 204 205
C192S K C C S T L Q R L S A205S
162 166 189 192 200 201 202 203 204 205
KCCC/RSSS R S S S T L Q R L T A205T
162 166 189 192 200 201 202 203 204 205
ΔKCCC
Deletion 162-192
C
fA3Z2bZ3 + Vif
fA3Z2bZ3-FLAG
Vif-HA
Merge
Vif alone
No Vif
WT
WT
TLQ/AAA
TLQ/AAA
ΔKCCC
ΔKCCC
KCCC/RSSS
KCCC/RSSS
D
Empty vector
WT FIV Vif
TLQ/AAA
TLQ/TAQ
A205L
A205S
A205T
HA (Vif)
Tubulin
Empty vector
WT FIV Vif
K162R
C166S
C189S
C192S
ΔKCCC
KCCC/RSSS
HA (Vif)
Tubulin

Fig. 1

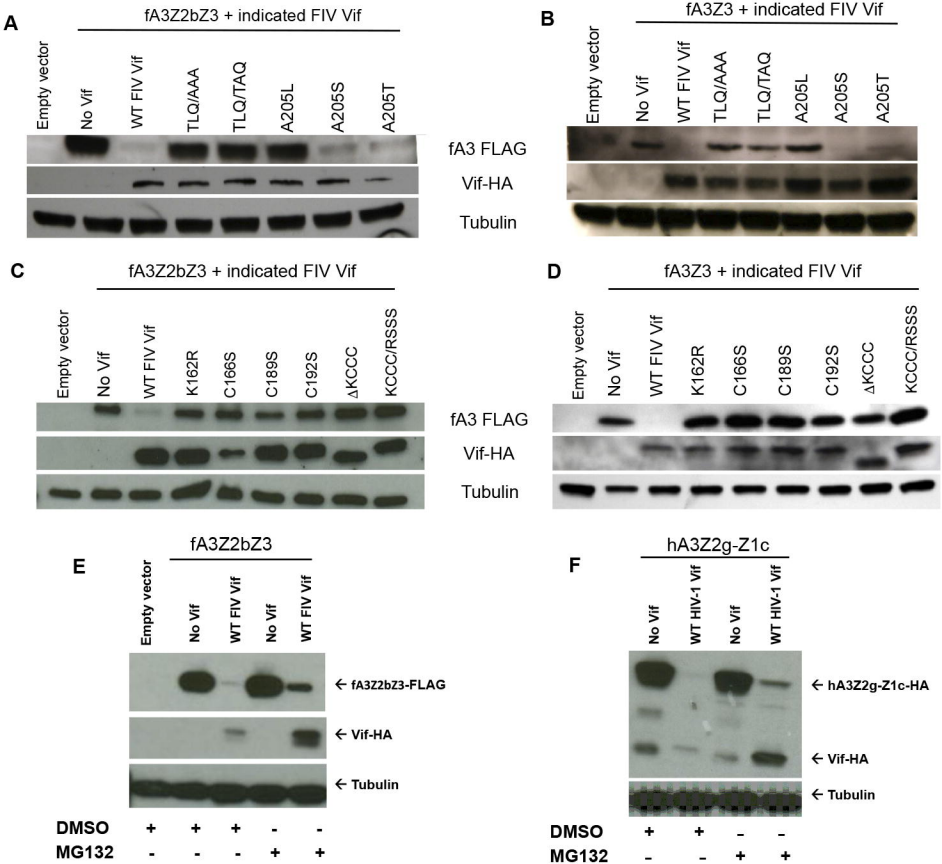
A
fA3Z2bZ3 + indicated FIV Vif
Empty vector
No Vif
WT FIV Vif
TLQ/AAA
TLQ/TAQ
A205L
A205S
A205T
fA3 FLAG
Vif-HA
Tubulin
B
fA3Z3 + indicated FIV Vif
Empty vector
No Vif
WT FIV Vif
TLQ/AAA
TLQ/TAQ
A205L
A205S
A205T
C
fA3Z2bZ3 + indicated FIV Vif
Empty vector
No Vif
WT FIV Vif
K162R
C166S
C189S
C192S
ΔKCCC
KCCC/RSSS
fA3 FLAG
Vif-HA
Tubulin
D
fA3Z3 + indicated FIV Vif
Empty vector
No Vif
WT FIV Vif
K162R
C166S
C189S
C192S
ΔKCCC
KCCC/RSSS
E
fA3Z2bZ3
Empty vector
No Vif
WT FIV Vif
No Vif
WT FIV Vif
← fA3Z2bZ3-FLAG
← Vif-HA
← Tubulin
DMSO + + + - -
MG132 - - - + +
F
hA3Z2g-Z1c
No Vif
WT HIV-1 Vif
No Vif
WT HIV-1 Vif
← hA3Z2g-Z1c-HA
← Vif-HA
← Tubulin
DMSO + + - -
MG132 - - + +

Fig. 2

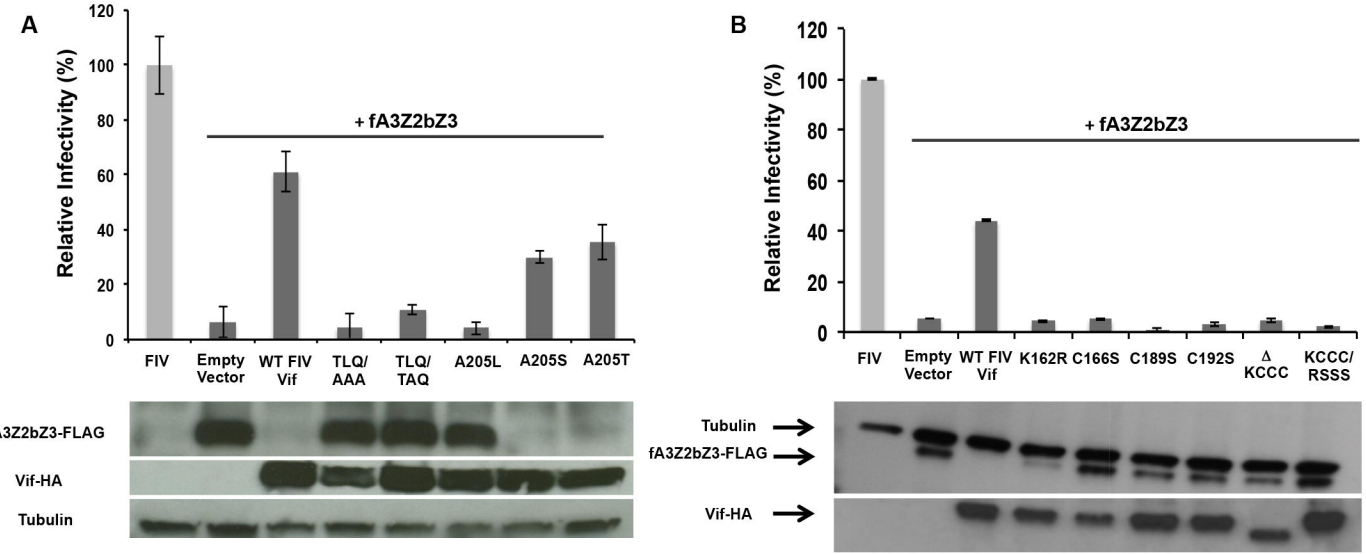
A
Relative Infectivity (%)
120
100
80
60
40
20
0
+ fA3Z2bZ3
FIV
Empty Vector
WT FIV Vif
TLQ/ AAA
TLQ/ TAQ
A205L
A205S
A205T
fA3Z2bZ3-FLAG
Vif-HA
Tubulin
B
Relative Infectivity (%)
120
100
80
60
40
20
0
+ fA3Z2bZ3
FIV
Empty Vector
WT FIV Vif
K162R
C166S
C189S
C192S
Δ KCCC
KCCC/ RSSS
Tubulin
fA3Z2bZ3-FLAG
Vif-HA

Fig. 3

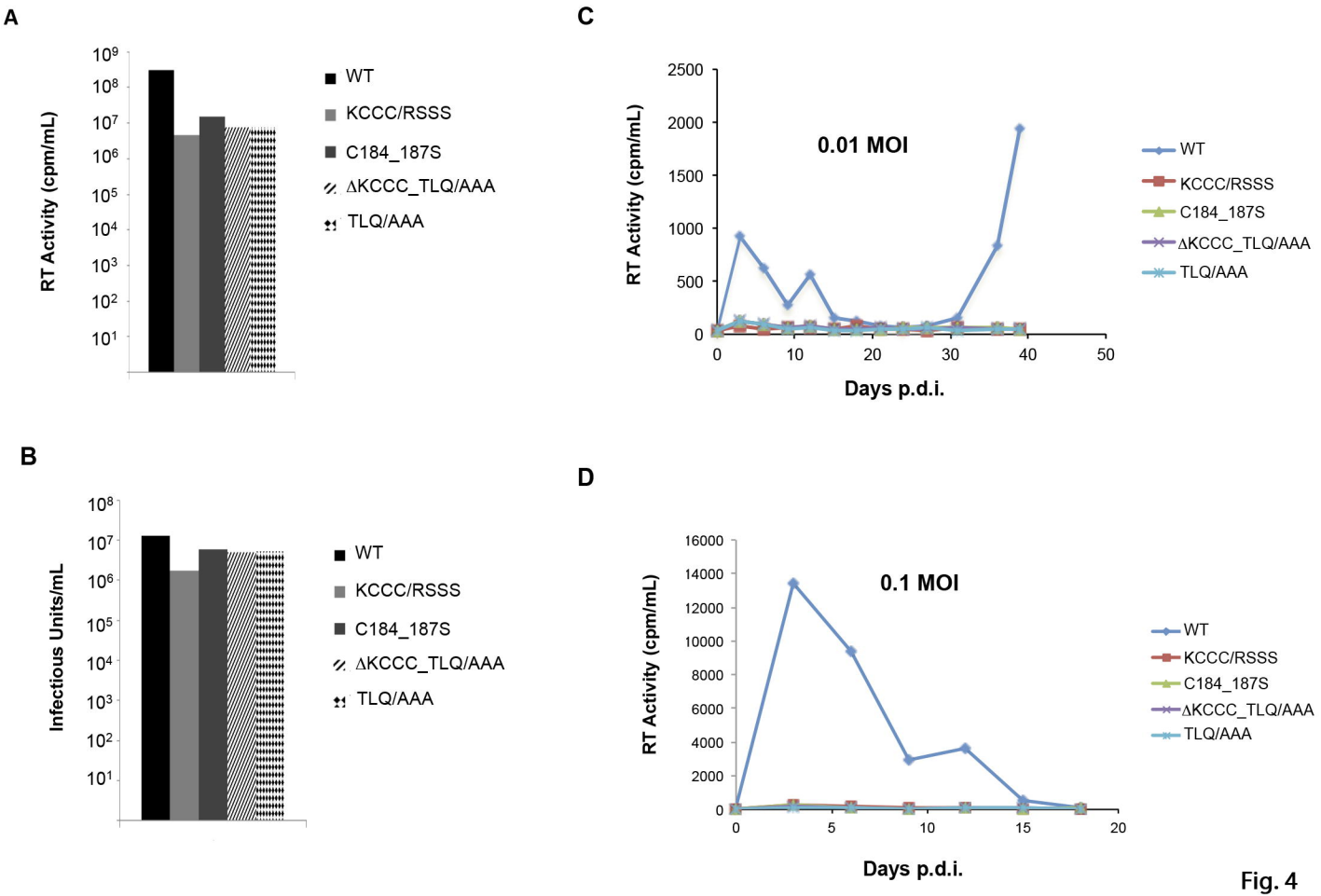
A
RT Activity (cpm/mL)
10^9
10^8
10^7
10^6
10^5
10^4
10^3
10^2
10^1
WT
KCCC/RSSS
C184_187S
ΔKCCC_TLQ/AAA
TLQ/AAA
B
Infectious Units/mL
10^8
10^7
10^6
10^5
10^4
10^3
10^2
10^1
WT
KCCC/RSSS
C184_187S
ΔKCCC_TLQ/AAA
TLQ/AAA
C
0.01 MOI
RT Activity (cpm/mL)
2500
2000
1500
1000
500
0
0
10
20
30
40
50
Days p.d.i.
WT
KCCC/RSSS
C184_187S
ΔKCCC_TLQ/AAA
TLQ/AAA
D
0.1 MOI
RT Activity (cpm/mL)
16000
14000
12000
10000
8000
6000
4000
2000
0
0
5
10
15
20
Days p.d.i.
WT
KCCC/RSSS
C184_187S
ΔKCCC_TLQ/AAA
TLQ/AAA

Fig. 4

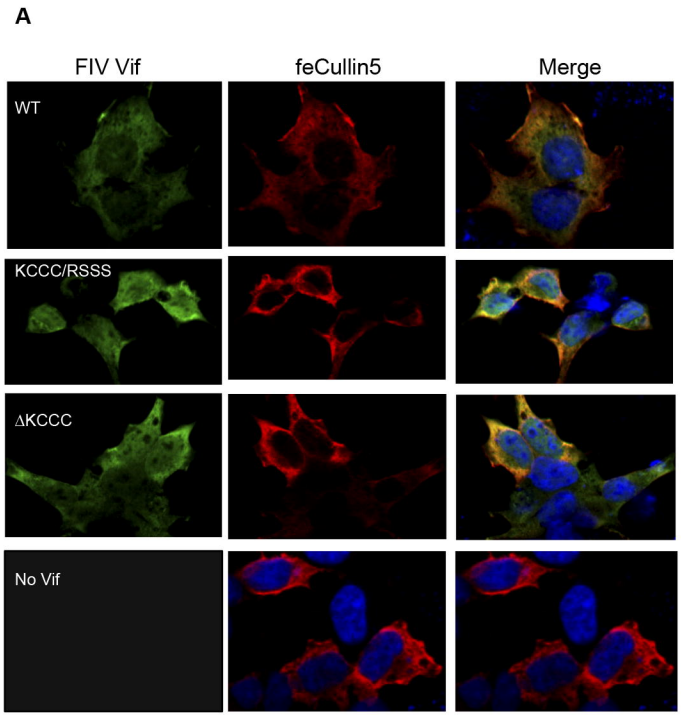
A
FIV Vif
feCullin5
Merge
WT
KCCC/RSSS
ΔKCCC
No Vif

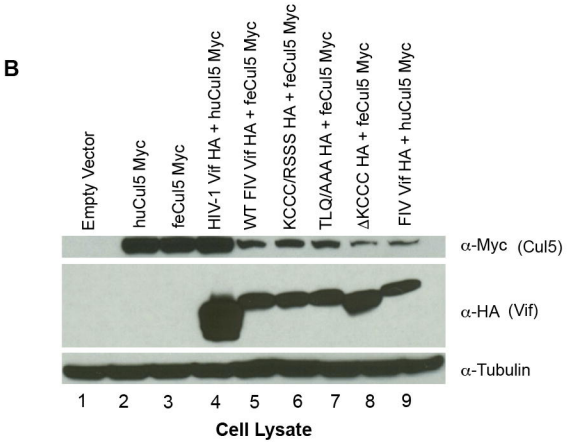
B
Empty Vector
huCul5 Myc
feCul5 Myc
HIV-1 Vif HA + huCul5 Myc
WT FIV Vif HA + feCul5 Myc
KCCC/RSSS HA + feCul5 Myc
TLQ/AAA HA + feCul5 Myc
ΔKCCC HA + feCul5 Myc
FIV Vif HA + huCul5 Myc
α-Myc (Cul5)
α-HA (Vif)
α-Tubulin
1 2 3 4 5 6 7 8 9
Cell Lysate

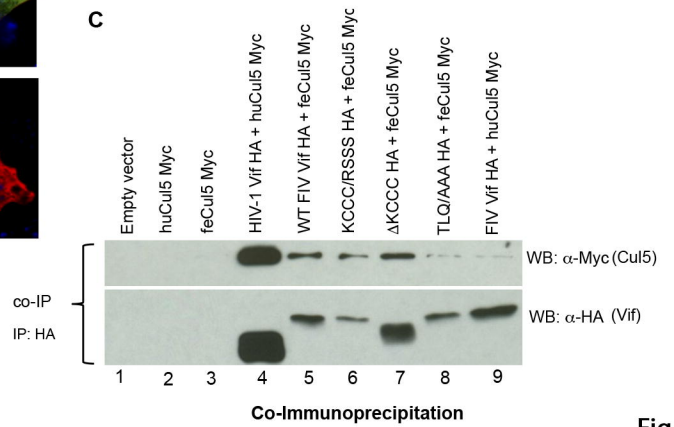
C
Empty vector
huCul5 Myc
feCul5 Myc
HIV-1 Vif HA + huCul5 Myc
WT FIV Vif HA + feCul5 Myc
KCCC/RSSS HA + feCul5 Myc
ΔKCCC HA + feCul5 Myc
TLQ/AAA HA + feCul5 Myc
FIV Vif HA + huCul5 Myc
co-IP
IP: HA
WB: α-Myc (Cul5)
WB: α-HA (Vif)
1 2 3 4 5 6 7 8 9
Co-Immunoprecipitation

Fig. 5

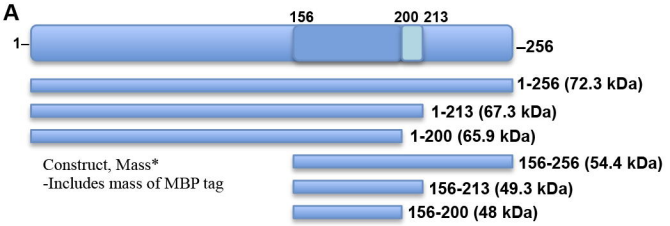

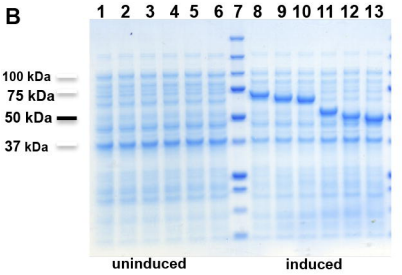

Lane Description
1. 1-256, t_0
2. 1-213, t_0
3. 1-200, t_0
4. 156-256, t_0
5. 156-213, t_0
6. 156-200, t_0
7. Marker
8. 1-256, t_f
9. 1-213, t_f
10. 1-200, t_f
11. 156-256, t_f
12. 156-213, t_f
13. 156-200, t_f

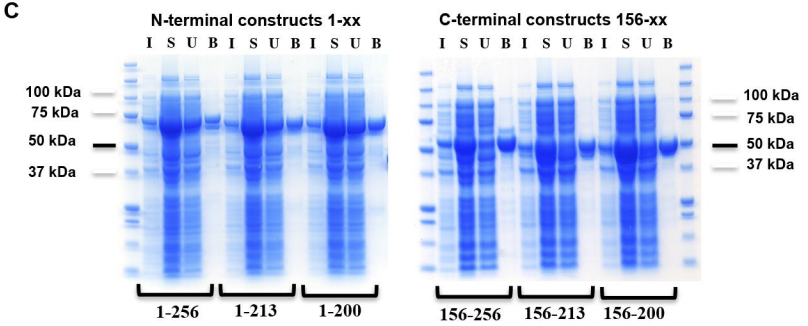

D

Construct	1^0 Peak	Comment
1-256	7.5 mL	Aggregate
1-213	7.5 mL	Aggregate
1-200	7.5 mL	Aggregate
156-256	10 mL	Broad Peak
156-213	17 mL	Monomer
156-200	17 mL	Monomer

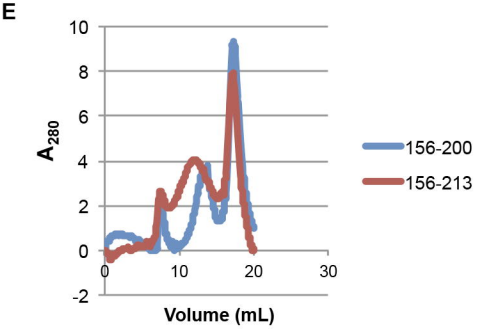

Fig. 6

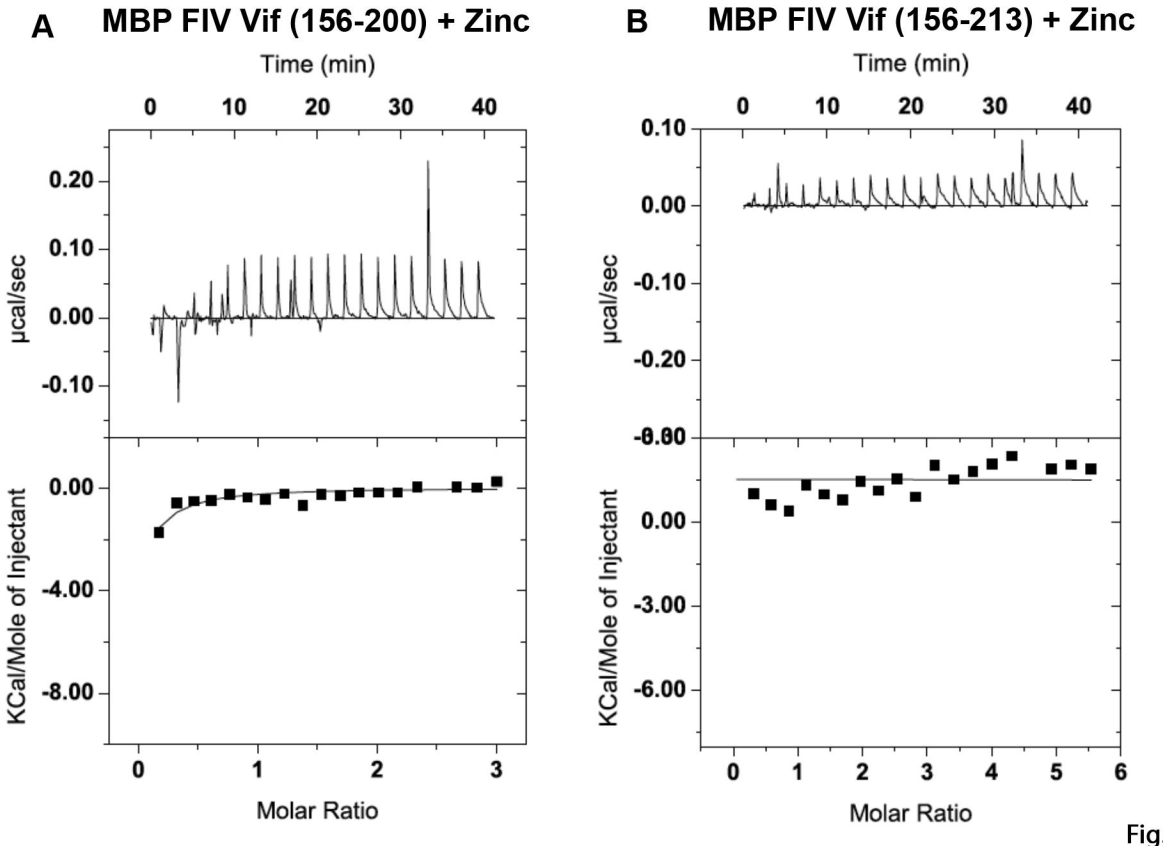
A
MBP FIV Vif (156-200) + Zinc
Time (min)
0
10
20
30
40
0.20
0.10
0.00
-0.10
µcal/sec
0.00
-4.00
-8.00
KCal/Mole of Injectant
0
1
2
3
Molar Ratio
B
MBP FIV Vif (156-213) + Zinc
Time (min)
0
10
20
30
40
0.10
0.00
-0.10
-0.20
µcal/sec
0.00
-3.00
-6.00
KCal/Mole of Injectant
0
1
2
3
4
5
6
Molar Ratio

Fig. 7